Hindawi Publishing Corporation
Journal of Nanomaterials
Volume 2009, Article ID 879016, 5 pages
doi:10.1155/2009/879016

Research Article

Formation and Characterization of TiO_2/CNT Nanomaterials Dried under Supergravity Conditions

Minerva Vargas,[1] Marina E. Rincón,[2] and Eduardo Ramos[2]

[1] *Departamento de Metalmecánica, Instituto Tecnológico de Zacatepec, Calzada Tecnológico 27, 62780 Zacatepec, MOR, Mexico*
[2] *Centro de Investigación en Energía, Universidad Nacional Autónoma de México, Privada Xochicalco s/n, Col. Centro, 62580 Temixco, MOR, Mexico*

Correspondence should be addressed to Minerva Vargas, mvv@cie.unam.mx

Received 7 May 2008; Accepted 12 January 2009

Recommended by Donald Bansleben

The elaboration of bilayer TiO_2/CNT films dried under terrestrial gravity conditions (g) and on a centrifuge with $1.3g$ and $7g$ is reported. The changes in microstructure and thickness of these coatings under supergravity environment cause a red-shift tendency in the optical properties at increasing values of acceleration. Experiments of a drop under enhanced gravity force in the range of $3.7 < \text{Bo}$ (bond number) < 51.5 suggest the incomplete elimination of surfactant-water molecules in the TiO_2/CNT bilayer film. Increasing acceleration up to $14g$ will widen the optical differences found, proving the layer-by-layer solution-chemical method in combination with these drying protocols, an alternative to produce thickness-sensitive solar-selective absorbing coatings.

1. Introduction

Materials processing in centrifuges have two interesting motivations: first, opportunities for production of unique and improved materials that cannot be prepared under normal earth conditions or in space; second, such research improves our understanding of the influence of acceleration and thermophysical mechanisms on materials processing. Research on processing materials in high gravity has been increased in the last twenty years due to the fact that even a modest increase in acceleration gives dramatic effects on the physical properties of the materials [1]. Few examples are the improved compositional homogeneity of semiconductors [2, 3]: the increased nucleation rates, growth rates, and coverage area for diamond film deposition [4, 5]; the improved quality of protein and high-energy crystals [6]; the large-scale production of nanoparticles [7, 8].

On the other hand, mesoporous materials based on carbon nanotubes (CNTs) are of great interest because they possess many of the unique electronic and mechanical properties of the carbon nanotubes [9]. In these complex materials, dispersion and pore penetration are the qualities affecting conductivity, optical properties, and strength. Recently, bilayer and composites systems based on TiO_2/CNT are being investigated as sensors [10], photocatalysts [11], and spectral selective absorbing films [12]. In this work, we use stainless steel substrates coated with sol-gel mesoporous titania, followed by a cast layer of carbon nanotube-surfactant film to create a tandem system consisting of a reflector/porous matrix/absorbing layer. The optical properties of this tandem system were reported to be sensitive to the morphology resulting from the annealing process [12]. Here, instead of thermally drying the samples, we proposed drying under terrestrial gravity conditions (g) and also under acceleration in the range of $1g$ to $7g$. Moreover, to better understand the drying process, images of a drop under enhanced gravity force in the range of $3.7 < \text{Bo}$ (bond number) < 51.5 will be presented and discussed in the context of the TiO_2/CNT results.

2. Experimental

The experimental methodology consists of three parts: sample preparation, drying, and characterization.

2.1. Sample Preparation

2.1.1. Mesoporous TiO_2 Film. This is done on $2\,\text{cm} \times 8\,\text{cm}$ mirror-polished stainless steel substrates by sequential

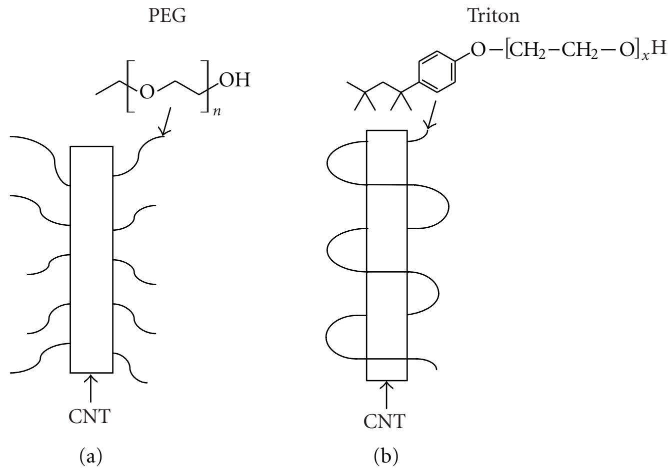

Scheme 1: Interactions between PEG/Triton and carbon nanotubes-rich soot: (a) covalent bonding through the functionality of the carbon surface; (b) noncovalent wrapping of the carbon surface.

immersion/drying cycles of the substrates in a 2-propanol solution of titanium tetraisopropoxide and polyethylene glycol (PEG, Mn:400). The approximate concentration of TiO_2 in the solution is 20 mg/mL. A complete description of this procedure can be found elsewhere [12]. After TiO_2 deposition, the coated substrates are air annealed at 450°C for 15 minutes.

2.1.2. Deposition of Carbon Nanotubes. The carbon nanotubes were provided by Professor Gilles Flamant from Processes, Materials and Solar Energy Laboratory (PROMES-CNRS), France. They are nanotube-rich soot that has been elaborated in a 50 kW solar reactor operating at the focus of the solar furnace at CNRS, Odeillo, France. A suspension made of 3 g Triton X-100, 3 g PEG, and 0.05 g of carbon nanotubes was prepared (Scheme 1). The suspension was sonified for 90 minutes, and then 30 mL of 2-propanol were added and centrifuged again for 30 minutes. The supernatant liquid was discarded and the nanotubes redissolved in water and centrifuged again. In the third centrifugation, the nanotubes could no longer be precipitated, and the ink was stable for weeks. A small volume of the carbon nanotubes emulsion (0.05 mL) was cast and let dry for 24 hours on the TiO_2 coated substrates.

2.2. Drying Process

2.2.1. TiO_2/CNT Films. Two drying protocols were designed: in the first, witness samples were dried under the influence of terrestrial gravity, lying flat on a horizontal plane; in the second protocol, wet samples (2 hours after deposition) were mounted on a centrifuge and spun during 50 minutes at rates of 22 rpm and 60 rpm. The distance of the samples to the centrifuge rotation axis was 170 cm which amounted to a centrifugal acceleration of $1.2g$ (samples spun at 22 rpm) and $6.8g$ (samples spun at 60 rpm). The magnitudes of the total acceleration a and gravity plus centrifugal force were $1.3g$ (at 22 rpm) and $6.9g$ (at 60 rpm). The samples were mounted at one end of one arm of the centrifuge such that they were always perpendicular with respect to the total acceleration. This is shown schematically in Figure 1. A more detailed description of the centrifuge can be found elsewhere [13].

2.2.2. Drop Behavior in a Centrifuge. In order to assess the gravity force effects on the shape of a static drop sitting on a solid surface, experiments were performed in the range of $3.7 <$ Bo (bond number) < 25.7. Here, $\mathrm{Bo} = a\rho d^2/\gamma$, where a is the total acceleration, ρ is the fluid density, d is the drop footprint diameter, which for our experiment was 5.2 mm, and γ is the fluid surface tension. The bond number is a relation between gravity and surface tension effects. Another important parameter is the capillary length $\kappa^{-1} = (\gamma/a\rho)^{1/2}$, which gives information about the drop shape. Images were captured by an experimental arrangement integrated by a video camera (Sony CCD-TRV87), a beam-splitter cube, and two low-intensity 20 W lamps to avoid evaporation. The changes on drop height and area when the water drop was subjected to centrifugation were analyzed in the interval of $1g < a < 14g$. Image views of the side and the bottom of the drop were captured (see Figure 2), digitized, and processed by a Visual Builder V2.0 from (National Instruments, Austin, Tex, USA).

2.3. Films Characterization. Film thickness was measured with an alpha-step system. The microstructure was obtained by scanning electron microscopy (JEOL model JMS-5600LV) and the optical properties with a Shimadzu UV-3101PC spectrophotometer equipped with an integration sphere. An aluminum mirror was used as a reference mirror for the measurements of specular reflectance, while barium sulfate was used as a reference coating for the measurements of diffuse reflectance.

3. Results and Discussion

3.1. TiO_2/CNTS-PEG400 Coatings. Figure 3 shows the film thickness of TiO_2/CNTS-PEG400 coatings after centrifugation. Measurements were taken along the longitudinal and

Figure 1: (a) Centrifuge used for drying the samples under supergravity conditions. (b) Articulated boat holding the substrates. g: Gravity acceleration; $\omega^2 R$: Centrifugal acceleration; ω: Angular velocity; R: Distance from the sample to the rotation axis; a: Total acceleration.

Figure 2: Sketch of the side and bottom views of a static drop captured by a video camera.

transversal axes at the positions indicated in the left side of the figure. The samples were rested for two hours at ambient conditions prior to the mounting in the centrifuge where they were spun for 50 minutes at 60 rpm. From the figure, it is clear that a slight mass enrichment is found at position 3, although in general for this drying protocol the films have uniform thickness with the values of the longitudinal axis following closely the ones found for the transversal axis. Samples dried at $1g$ for more than 24 hours had an average thickness value of 1.68 μm, which is almost 50% higher than the average value of Figure 3. It is interesting to notice that although the spun coatings look dried, they are approximately twice as thick as those reported in previous work, where the films were thermally dried [12]. Therefore, it is reasonable to assume that although an important amount of PEG400 was removed at $7g$, some remains inside the porous films. Apparently, the interaction between CNTs and the surfactants can be broken during annealing but not necessarily under centrifugation at $7g$.

The microstructure of the tandem system (stainless steel/mesoporous TiO_2/CNTS-PEG400) was obtained by scanning electron microscopy at various magnifications. Figure 4 shows images of films dried at ambient conditions (Figure 4(a)) and at 60 rpm (Figure 4(b)). Indicating that, under rotation, there is redistribution of the mobile phase made up by carbon nanotubes soot and PEG400/Triton X-100; the films are still wet, and the features of the carbon nanotubes soot are not resolvable. Additionally, the comparison of SEM images (not shown) of films dried under different angular velocities but similar rotation time shows the TiO_2 layer as a background collection of nanoparticles,

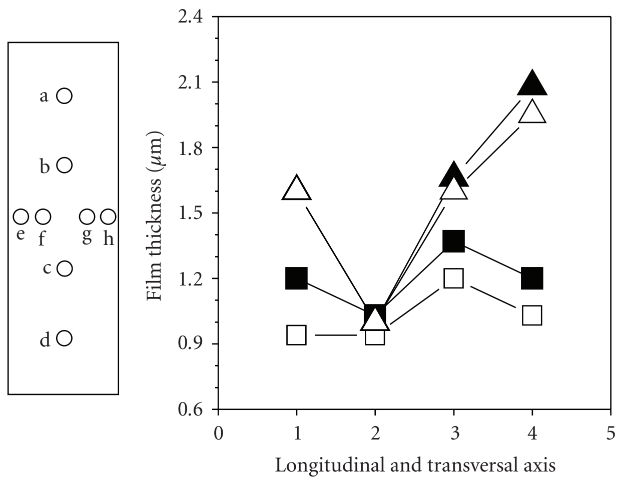

Figure 3: Thickness of films dried at $a = 1g$ (triangles) and $a = 7g$ (squares). Positions (a–d) selected along the longitudinal axis correspond to (1–4) (solid symbol). Positions (e–h) along the transversal axis correspond to (1–4) (empty symbol).

while the appearance of the CNTS-PEG400 layer depends on the angular velocity.

Figure 5 shows the reflectance of the stainless steel mesoporous TiO_2/CNTS-PEG400 system as a function of light wavelength in the interval of 0.25 μm to 22 μm. The curves correspond to total reflectance in the UV-visible-near infrared region. The total reflectance of the samples centrifuged either at 22 rpm or 60 rpm shows good reproducibility (empty and solid symbols). Interestingly, the differences due to the drying protocol, terrestrial or supergravity, are clearly observed at 60 rpm but not at 22 rpm angular velocity. The reflectance for tandem systems dried under terrestrial gravity for 24 hours is also shown in the figure (red curve). It resembles the reflectance curve of the coatings spun at 22 rpm. In general, all the systems dried at 60 rpm give lower values of reflectance than those spun at 22 rpm, in agreement with a thinner and more uniform distribution of the absorbing layer. Although these films still require optimization, our results indicate that larger angular velocities ($14g$) and/or superior centrifugation time can

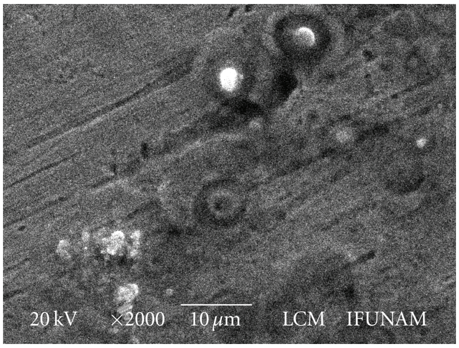

(a)

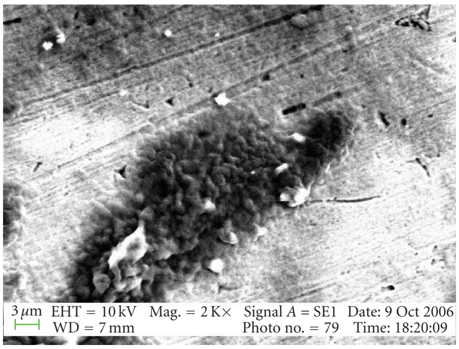

(b)

FIGURE 4: SEM images of mesoporous TiO_2/CNTS-PEG400 tandem films: (a) dried at ambient conditions and (b) at 60 rpm.

yield an even thinner and well-dispersed pigment, increasing the absorbance of the films in the near infrared region. Nevertheless, the present results are in the range of solution-chemically derived spectrally selective absorbers with more complex structures [14].

3.2. Drop Behavior in a Centrifuge. To better understand the drying process, images of a water drop under enhanced gravity force in the range of $3.7 < \mathrm{Bo} < 51.5$ are presented in Figure 6. The sequence describes the drop under supergravity environments, from $1g$ to $14g$. In these experiments, the initial drop volume was 20 μL, the bottom area 21 mm^2, and the height 1.5 mm. From the figure, it is clear that changes occur even at $1.7g$. The normalized height of the drop (h/ho, where ho is the height of the drop at $1g$) decreased with increasing acceleration as shown by the relation plotted in Figure 7.

The theory for large drops predicts $h \sim a^{-0.5}$ [15, 16], but the trend indicated by the points in Figure 7 indicates that the height drops faster when the total acceleration increases from $1g$ to $14g$. Although the discrepancy can be attributed to the changes in the contact angle and evaporation, a full analysis is outside the scope of the present work, particularly because the mechanisms that govern the hydrodynamics controlling wetting or evolution of drop into films are still not fully understood. Nevertheless, the shape of the drop follows the condition expected for drops with flattened tops ($d > \kappa^{-1}$) at all a, assuring the formation of thin films.

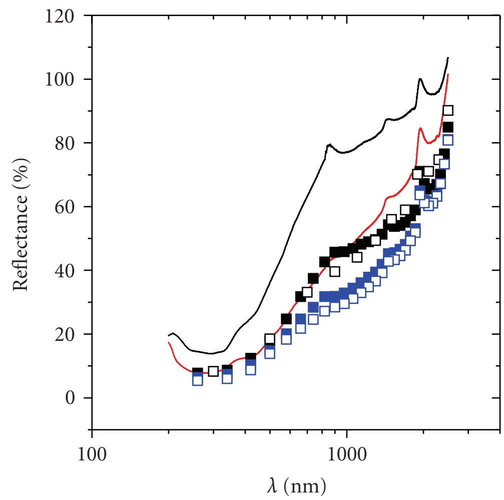

FIGURE 5: Spectrally selective stainless steel/TiO_2/CNTS-PEG400 system as a function of the angular velocity (22 rpm black symbols and 60 rpm blue symbols). Empty symbols correspond to duplicate experiments. The solid red line represents the system dried under terrestrial gravity on a 5° tilted plane. The black line corresponds to the reflectance curve of stainless steel/mesoporus TiO_2.

The results presented in Figures 6 and 7 agree with the observation that TiO_2/CNTS-PEG400 coatings are still thick at $7g$ but can be substantially thin out at $14g$. In this context, we conclude that thickness-sensitive solar-selective absorbing coatings can be prepared under supergravity environment in the range of $1g$ to $14g$.

4. Conclusions

The layer-by-layer solution-chemical method in combination with some of the drying protocols investigated in this work has proved successful in producing coatings with good spectrally selective properties. Among the issues learned, we found that surfactant polymers used as CNTs dispersant are not completely eliminated under the present centrifugal force, requiring either thermal treatment or higher a values. Nevertheless, the microstructure and thickness changes of these coatings under supergravity environment in the range of $1g$ to $7g$ cause a red-shift tendency at increasing values of a, which could constitute an alternative method to produce thickness-sensitive solar-selective absorbing coatings. Further work is in progress varying the centrifugation time and the elimination/carbonization of the remaining surfactants to improve even more the absorbance of these films.

Acknowledgments

The authors would like to thank Dr. C. Menchaca CIICAP-UAEM for SEM images and M. Sánchez-Tizapa and G. Hernández-Cruz for technical assistance. Financial support from Projects CONACyT (49100), (25116), and DGAPA-UNAM (IN111106) are gratefully acknowledged.

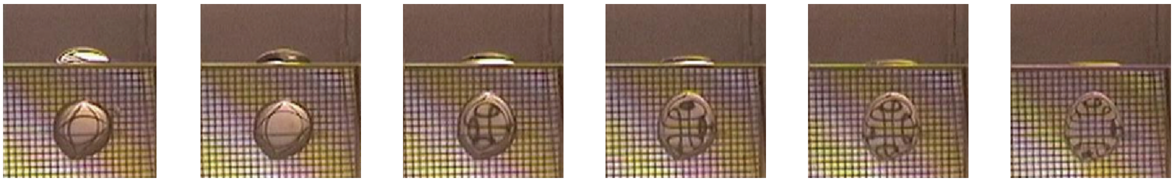

FIGURE 6: Water drop at different total accelerations: (a) 1.0g, (b) 1.7g, (c) 3.7g, (d) 6.9g, (e) 10.4g, and (f) 14g.

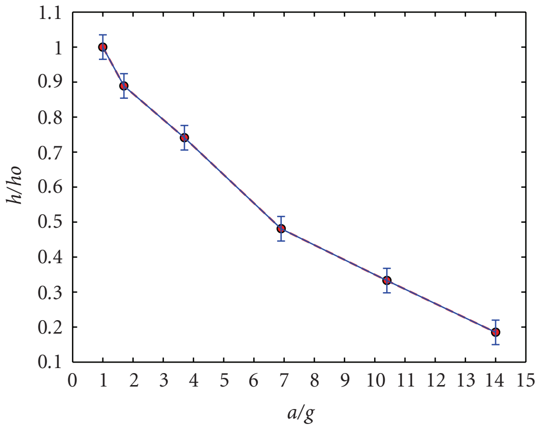

FIGURE 7: Normalized height of the drop as a function of total acceleration. The error bars correspond to the instrument uncertainty.

References

[1] L. Regel and W. Wilcox, "Introduction to materials processing in large centrifuges," in *Materials Processing in High Gravity*, pp. 1–16, Plenum Press, New York, NY, USA, 1994.

[2] W. C. Yu, Z. B. Chen, W. T. Hsu, B. Roux, T. P. Lyubimova, and C. W. Lan, "Effects of angular vibration on the flow, segregation, and interface morphology in vertical Bridgman crystal growth," *International Journal of Heat and Mass Transfer*, vol. 50, no. 1-2, pp. 58–66, 2007.

[3] D. N. Riahi, "Effects of Coriolis and centrifugal forces on the melt during directional solidification of a binary alloy," in *Materials Processing in High Gravity*, pp. 133–138, Plenum Press, New York, NY, USA, 1994.

[4] F. Tappero, Y. Abe, Y. Takagi, Y. Tanaka, and G. Maizza, "Wireless optical diagnostic apparatus for analyzing diamond thin film CVD process under high gravity conditions," *Diamond and Related Materials*, vol. 13, no. 11-12, pp. 2063–2070, 2004.

[5] M. Nakasato, T. Suzuki, Y. Nagasaka, Y. Abe, S. Bellingeri, and G. Maizza, "Diamond synthesized DC-plasma CVD at high gravity," in *Processing by Centrifugation*, L. L. Regel and W. R. Wilcox, Eds., pp. 107–112, Kluwer Academic/Plenum Publishers, New York, NY, USA, 2001.

[6] J. Behle and O. Ristay, "Analytical ultracentrifugation: a valuable tool to recognize crystallization conditions of proteins," in *Processing by Centrifugation*, L. L. Regel and W. R. Wilcox, Eds., pp. 61–70, Kluwer Academic/Plenum Publishers, New York, NY, USA, 2001.

[7] J. Chen, Y. Li, Y. Wang, J. Yun, and D. Cao, "Preparation and characterization of zinc sulfide nanoparticles under high-gravity environment," *Materials Research Bulletin*, vol. 39, no. 2, pp. 185–194, 2004.

[8] Y. Wang and J. Chang, "Synthesis and application of nanoparticles by multiphase reactive precipitation in a high-gravity reactor II: modeling," in *Processing by Centrifugation*, L. L. Regel and W. R. Wilcox, Eds., pp. 29–36, Kluwer Academic/Plenum Publishers, New York, NY, USA, 2001.

[9] E. Kymakis, I. Alexandou, and G. A. J. Amaratunga, "Single-walled carbon nanotube-polymer composites: electrical, optical and structural investigation," *Synthetic Metals*, vol. 127, no. 1–3, pp. 59–62, 2002.

[10] R. A. Guirado-López, M. Sánchez, and M. E. Rincón, "Interaction of acetone molecules with carbon-nanotube-supported TiO_2 nanoparticles: possible applications as room temperature molecular sensitive coatings," *Journal of Physical Chemistry C*, vol. 111, no. 1, pp. 57–65, 2007.

[11] G. An, W. Ma, Z. Sun, et al., "Preparation of titania/carbon nanotube composites using supercritical ethanol and their photocatalytic activity for phenol degradation under visible light irradiation," *Carbon*, vol. 45, no. 9, pp. 1795–1801, 2007.

[12] M. E. Rincón, J. D. Molina, M. Sánchez, C. Arancibia, and E. García, "Optical characterization of tandem absorber/reflector systems based on titanium oxide-carbon coatings," *Solar Energy Materials and Solar Cells*, vol. 91, no. 15-16, pp. 1421–1425, 2007.

[13] M. Vargas, E. Ramos, G. Ascanio, R. Espejel, G. Esquivel, and G. Hernández-Cruz, "A centrifuge for studies of fluid dynamics phenomena in a rotating frame of reference," *Revista Mexicana de Fisica*, vol. 48, no. 3, pp. 255–266, 2002.

[14] T. K. Boström, E. Wäckelgård, and G. Westin, "Durability tests of solution-chemically derived spectrally selective absorbers," *Solar Energy Materials and Solar Cells*, vol. 89, no. 2-3, pp. 197–207, 2005.

[15] F. Brochard-Wyart, H. Hervet, C. Redon, and F. Rondelez, "Spreading of "heavy" droplets: I. Theory," *Journal of Colloid And Interface Science*, vol. 142, no. 2, pp. 518–527, 1991.

[16] C. Isenberg, *The Science of Soap Films and Soap Bubbles*, Dover, New York, NY, USA, 1992.